Materials Advances

ROYAL SOCIETY OF CHEMISTRY

PAPER

View Article Online
View Journal | View Issue

Cite this: *Mater. Adv.*, 2021, 2, 5443

A ruthenium-inserted hydrotalcite (Ru-HT) heterogeneous catalyst: kinetic studies on the selective hydrogenation of carbon dioxide to formic acid†

Minaxi S. Maru, *[abc] Sanwala Ram,[ad] Noor-ul H. Khan [ad] and Ram S. Shukla*[ad]

Kinetic studies have been carried out for the base-free hydrogenation of CO_2 to formic acid using a heterogeneous ruthenium-inserted hydrotalcite (Ru-HT) catalyst. An impressive turnover number (TON = 11 389) was achieved for formic acid under the optimized reaction conditions using a methanol : water mixture as the solvent (5 : 1, v/v) with 60 bar total pressure at 60 °C for 24 hours. The rates were determined directly in terms of the formation of formic acid with time. Kinetics were performed by carrying out experiments concerning the amount of catalyst, the individual partial pressures of CO_2 and H_2, the total pressure, temperature, agitation speed, reaction volume and v/v ratio of the mixed solvent. The rate of formic acid formation was first order on the amount of catalyst and partial pressures of CO_2 and H_2. The best reaction conditions achieved from the kinetic parametric optimization were: 100 mg catalyst, 30 bar pCO_2, 30 bar pH_2, 60 °C temperature, 800 rpm agitation speed and methanol–water (5 : 1, v/v) solvent. The computed activation parameters obtained from the temperature-dependent rate of formic acid formation were E_a = 34.5 ± 2.5 kJ mol^{-1}, $\Delta H^{\#}$ = 32 ± 2.5 kJ mol^{-1} and $\Delta S^{\#}$ = −384 ± 5 J deg^{-1} mol^{-1}. The presence of water in the mixed solvent effectively enhanced the reaction rate, which is characteristically observed due to its molecular effect. Two mechanistic routes for CO_2 hydrogenation to formic acid are proposed and discussed based on the kinetic and experimental observations. The studied parameters were found to be significantly effective to increase the rate of reaction appreciably.

Received 12th May 2021,
Accepted 2nd July 2021

DOI: 10.1039/d1ma00431j

rsc.li/materials-advances

Introduction

Carbon dioxide (CO_2), a potent greenhouse gas produced mainly through the combustion of fossil fuels and deforestation, is significantly contributing to global warming. Although many ways are proposed to curtail or damp its emission into the atmosphere, one of attractive way is to convert it into useful chemicals due to its availability as a plentiful, cheap and non-toxic C-1 resource, specifically for formic acid as it is a renewable energy source for H_2 gas.[1] Formic acid is an essential intermediate and fundamental chemical feedstock in industrial organic chemistry because of its indispensable application in textile-making, dyeing, paper-making, the production of medicinal agents, tanning agents in the leather industry, as a preservative agent in livestock feed and as an important intermediate in chemical synthesis. Formic acid is the foremost chemical for the production of many basic organic compounds like ketones, aldehydes, amides and carboxylic acids *via* formate esters, which are also essential in the fragrance and perfumery industries.[2] The currently established commercial process for the synthesis of formic acid is *via* a two-step procedure, using toxic carbon monoxide at high pressure and high temperature. In the first step, the formation of methyl formate by the carbonylation of methanol occurs using 2.5% (w/w) sodium methoxide as the catalyst, where only 30% of the methanol is converted into methyl formate, whereas in the second step, the hydrolysis of methyl formate gives formic acid.[3] To avoid the use of toxic carbon monoxide, a promising and potential replacement for the production of formic acid is the direct hydrogenation of very abundant, inexpensive and nontoxic CO_2

[a] *Inorganic Materials and Catalysis Division, Council of Scientific and Industrial Research (CSIR), Central Salt and Marine Chemicals Research Institute, G. B. Marg, Bhavnagar, 364002, Gujarat, India. E-mail: dr.maru139@gmail.com*
[b] *Inorganic Chemistry Division, Department of Chemistry, Saurashtra University, Rajkot, 360005, Gujarat, India*
[c] *Department of Chemistry, Indian Institute of Teacher Education (IITE), Gandhinagar, 382016, Gujarat, India*
[d] *Academy of Scientific and Innovative Research (AcSIR), Council of Scientific and Industrial Research (CSIR), Central Salt and Marine Chemicals Research Institute, G. B. Marg, Bhavnagar, 364002, Gujarat, India*

† Electronic supplementary information (ESI) available. See DOI: 10.1039/d1ma00431j

using various transition metal-based homogeneous and heterogeneous catalysts.[4–7]

The greenhouse effect of CO_2 is the most environmentally concerning problem in the world; many actions have been taken to counteract the danger of it, and the general reduction of CO_2 emissions has been proposed so far. Among the feasible approaches to reducing CO_2 emissions, processes based on CO_2 recycling have attracted major scientific and technological interest.[8] Accordingly, the hydrogenation of CO_2 to formic acid is one of the best atom-inexpensive reactions that has engaged the focus of many researchers in the field of catalysis.[9,10] The enthalpy change values of the reactions for the direct hydration of CO and the direct hydrogenation of CO_2 are $\Delta H = -28.4$ kJ mol^{-1} and $\Delta H = -31.6$ kJ mol^{-1}, respectively, and these are close enough to suggest the replacement of CO with CO_2.[3] The direct synthesis of formic acid by CO_2 hydrogenation is thermodynamically unfavourable, associated with about $\Delta G^{\circ}_{298} = +33$ kJ mol^{-1}.[11] The global demand for formic acid is continuously growing, particularly from the perspective of a renewable energy hydrogen source, and its production *via* the direct catalytic hydrogenation of CO_2 without the use of a base is considerably more sustainable in comparison with the existing reaction routes.

The utilization of CO and CO_2 for their conversions into industrially important value-added chemicals has been a focus of our research using heterogeneous catalytic systems since 2006. Recently, we have developed Cu-, Co-, Ru-, and Rh-based heterogeneous catalysts, which were found to be efficient for the selective hydrogenation of CO_2 to formic acid/formate and achieved remarkable results for formic acid/formate in terms of the CO_2 conversion and product selectivity, with astonishing turnover numbers.[12–14] A series of supported Rh complexes as efficient heterogeneous catalysts have been reported for the effective synthesis of alcohols from alkenes using carbon monoxide *via* hydroformylation, hydroaminomethylation, aldol condensation and stepwise hydrogenation.[15–22]

Among them, the hydrogenation of CO_2 to formic acid has been reported using hydrotalcite (HT) as a support material for the active catalytic system. Hydrotalcite belongs to the class of brucite-like layered double hydroxides with the general formula $Mg_{1-x}Al_x(CO_3^{2-})_{x/n}(OH_2)^{x+}\cdot m(H_2O)$ and it is an attractive inorganic base. Its catalytic activity can be improved through the intercalation of appropriate anions in the interlayer space, optimization of the Mg^{2+} and Al^{3+} molar ratio and activation of the final material at 450 °C. A number of metals can be grafted with hydrotalcite in its brucite-like layers *via* a co-precipitation method due to the isomorphic characteristic substitution of Mg^{2+} or Al^{3+} ions at the octahedral sites, which are considered to be the active sites for various organic transformations.[23,24]

Ruthenium-grafted hydrotalcite materials are reported to be highly active catalysts for oxidation, cyclocondensation, alkylation, methanation, and methanolysis reactions.[21,22a,25–29] Ru-containing materials and complexes have been the focus of investigations for the catalytic hydrogenation of CO_2 by molecular hydrogen, due to their potential favourable activity and selectivity for the formation of formic acid.[30] Very few reports are available on hydrotalcite for the hydrogenation of CO_2 for the production of formic acid and their kinetic studies. Kinetic studies for this kind of reaction have an important role in understanding the magnitude of the catalyst involvement towards the activation of CO_2 and H_2 molecules, the formation of a hydride and the insertion of CO_2 into such formed metal hydride bonds, thereby forming the formato intermediate resulting in the formation of the hydrogenated product. Investigations on kinetic aspects for the hydrogenation of CO_2 to formic acid are quite scarce, and few have been reported using homogeneous catalysts.[14,31,32] Further, some authors have reported kinetic studies for CO_2 hydrogenation to methanol over heterogeneous catalysts along with theoretical DFT studies.[33,34] Kinetic studies of a catalytic reaction are essential for achieving a systematic analysis of the catalytic system, so that improvements in its performance through the optimization of reaction parameters can be achieved to bring the product to a better and higher production level.[20]

Recently a heterogeneous Ru-hydrotalcite (Ru-HT)-based catalyst for CO_2 hydrogenation by molecular hydrogen for the selective synthesis of formic acid with a choice of ruthenium species was reported by our group.[13b] The catalyst was found to be effective for the hydrogenation and selective formation of formic acid at a moderate temperature without using any additional liquid or solid base, as is usually practised in this reaction. The soft solid base HT remarkably plays the dual role of support and of base. The activity and reusability of the Ru-HT catalyst were appreciable for the production of formic acid at a moderate temperature (60 °C) and 60 bar pressure (CO_2 and H_2).

The reactivity of the catalyst significantly depends on the kinetic factors in the catalytic process. The role of kinetic factors is very significant to monitor and control the reaction to the stage of the formation of product and optimisation of the reaction parameters, which can promise to bring the process to the commercial level.[35] Kinetic studies on the formation of formic acid are also instructive for improving the catalyst system and providing basic information on the design and scale-up of appropriate reactors. In view of the above, and since formic acid is a bulk chemical that is produced at a commercial level, there is a pressing need for detailed kinetic studies on the Ru-HT-catalysed heterogeneous hydrogenation of CO_2 to formic acid, so that the reaction parameters can be optimized under the employed reaction conditions. Thermodynamic insight is also substantiated in the present work for formic acid formation by determining activation parameters. The present work discusses the detailed kinetic investigations on the Ru-HT catalysed hydrogenation of CO_2 to formic acid according to the influence of the effective operating parameters: the amount of catalyst, the partial pressure of CO_2, the partial pressure of H_2, total pressure, temperature, agitation speed, the ratio of the methanol/water (v/v) solvent and the reaction volume, directly on the rate of selective formation of formic acid.

Experimental

Materials and methods

Hydrogen gas UHP/zero grade (99.9%) and carbon dioxide UHP/zero grade gas cylinders were purchased from Hydro Gas

India Pvt Ltd. Ruthenium trichloride [$RuCl_3{\cdot}xH_2O$] was acquired from Sigma-Aldrich, USA. Magnesium chloride [$MgCl_2{\cdot}6H_2O$; 98%], aluminum chloride [$AlCl_3{\cdot}9H_2O$; 98%], sodium nitrate [$NaNO_3$; 99.9%] and sodium hydroxide [NaOH; 99.9%] were purchased from S.D. Fine Chemicals Ltd, Mumbai, India and used as received. A.R. grade methanol was purchased from LobaChemie and was used without further purification. Double distilled Milli-Q deionized water was used for the synthesis of catalysts. The FT-IR spectra were recorded using a PerkinElmer Spectrum GX FT-IR system using KBr pellets in the mid-IR region. Powder X-ray diffraction (PXRD) patterns were obtained using a Rigaku MINIFLEX-II (FD 41521) powder X-ray diffractometer. The samples were scanned in the 2θ range of 10–80° using CuKα (λ = 1.54178 Å) radiation and a Ni filter. The textural analysis of the samples was carried out by nitrogen adsorption at 77.4 K using a Sorptometer (ASAP-2010, Micromeritics). X-Ray photoelectron spectroscopy (XPS) analysis was performed using an Omicron Nanotechnology system with monochromatic AlKα radiation through 1486.7 eV photon energy. FE-SEM (Field emission scanning electron microscopy) and EDX analysis were carried out using a JEOL JSM 7100F instrument at room temperature. Inductively coupled plasma (ICP) optical emission spectroscopy (ICPS-2000) was performed using a PerkinElmer Optima 2000 for the determination of the concentration of Ru element by using a Ru 240.3 analyte. The formic acid product was analyzed using a UV-vis spectrophotometer-P80+ in the wavelength range of 190–800 nm. These measurements were performed in 1 cm quartz cells using methanol as a standard. The UHPLC analysis was done using a SHIMADZU Nexera UHPLC system. Before HPLC analysis, all the samples and standards were filtered using an Axiva SFNY25XB nylon HPLC syringe filter (25 mm filter diameter/0.45 μm pore size) and left undiluted. Formic acid was separated using a HiQSilC18HS HPLC column (4.6 mm × 250 mm) operated at ambient temperature with an overall flow rate of 0.5 mL per minute of a 0.1% phosphoric acid mobile phase and detected using an SPD-M20A Prominence diode array UV detector set to 190 nm wavelength. The sample injection volume was 20 μL. The analysis was completed within 30 minutes, and data were recorded using the LabSolutions chromatography software.

Ru-HT catalyst preparation

The Ru-HT catalyst was prepared using a coprecipitation method at a constant pH, referring to the previously published method.[36] Solution A with $NaNO_3$ (0.079 mol) and solution B with $RuCl_3{\cdot}xH_2O$ (0.5 mmol), $Mg(NO_3)_2{\cdot}6H_2O$ (0.0522 mol) and $Al(NO_3)_3{\cdot}9H_2O$ (0.0144 mol) were each prepared in 50 mL of double distilled deionized water. Solution B was added dropwise to solution A at room temperature over around 45 minutes with continuous stirring and a constant pH of 10 was maintained using 1 M NaOH solution. The resulting mixture was then transferred into a Teflon coated stainless steel autoclave to age at 80 °C for 16 hours under autogenous water vapor pressure. The precipitate was filtered and washed with hot distilled water to remove the unreacted ions present in it. The solid material was dried at 80 °C, then ground and stored under vacuum as Ru-HT with a 3.5/1 molar ratio of Mg/Al in the hydrotalcite (HT). Ru-HT was activated at 450 °C for 4 hours in a muffle furnace. As the catalyst was recycled for up to 7 reaction cycles, the recycled catalyst was named RRu-HT.

CO_2 hydrogenation and kinetic measurements

The hydrogenation of CO_2 was done in a specially made high-pressure laboratory having safety precautions for using hydrogen and conducting reactions at high pressure and temperature, using an autoclave having 100 mL capacity. All operations involving the charging of gases were carried out in a well-ventilated fume hood. The reactor was charged with a known quantity of catalyst and a mixture of methanol and double distilled deionized water in the desired volume ratio (MeOH : H_2O, v/v), and the vessel was then sealed and flushed with CO_2 three times to remove air and was pressurized up to a final total desired pressure with CO_2/H_2 (1 : 1, p/p) at room temperature. The reactor was heated using a temperature controller to the desired temperature. Stirring was started at a fixed agitation speed (200–800 rpm) as the inside temperature of the reactor reached the employed temperature, which was considered to be the start of the reaction. After the desired reaction time, stirring and the heating were stopped and the reactor was allowed to cool to room temperature. The reactor was depressurized at room temperature and the vessel was opened and the reaction solution was collected by simple filtration to separate the catalyst.

The hydrogenation product was analyzed by HPLC and the concentration of the formed product was confirmed using a standard calibration curve plotted using area *vs.* formic acid concentration at the 190 nm wavelength. The formic acid peak was observed at a 19 minute retention time, which was completely detected as the same as that of the standard formic acid peak (Fig. S1, ESI†). The product was also analyzed spectrophotometrically using a chromotropic acid test and volumetrically by acid–base titration. A UV-vis P80+ spectrophotometer in the wavelength range of 190–800 nm was used for the analysis of the formic acid product. These measurements were performed in 1 cm quartz cells by taking methanol as a standard. Several repeated experiments were done to check the reproducibility of the reaction under identical reaction conditions, and the obtained results were found in the range of 3% variation.

For kinetic measurements, a series of kinetic experiments were carried out as a function of the amount of catalyst, the partial pressure of CO_2, partial pressure of H_2, total pressure, temperature, reaction volume and agitation speed for observing the effect of each individual parameter directly on the rate of formation of formic acid under identical employed reaction conditions. While varying an individual parameter, all the other parameters were kept constant. Aliquots were withdrawn from the reaction mixture at different desired time intervals and analysed to quantify the conversion in terms of the formation of formic acid in all the performed experiments.[16]

Results and discussion

Catalyst characterization

Morphology. The FE-SEM images (Fig. S2, ESI†) of Ru-HT show various small to large particles with layered stone-like structures (a very close observation displays a layer-like structure) with a rough surface. Fig. S2a and b (ESI†) display agglomeration of different size layered stones together with small particles on them, while in Fig. S2c and d (ESI†) formation of stones are clearly separated with a rough surface. These various size and shape layered stones are of hydrotalcite material and the small particles are because of the inserted ruthenium ion into it. The morphology of the recycled catalyst was checked after completion of all the seven catalytic cycles, when the catalyst started to drop the desirable conversion of formic acid and we observed that there is a difference in appearance between the surface of the fresh Ru-HT and the recycled Ru-HT (RRu-HT) (Fig. S2d–h, ESI†). The surface of Ru-HT is smoother than the surface of RRu-HT, maybe because of its use for seven catalytic cycles, which led to a decrease in product conversion followed by a tendency for destruction of the layered stone-like structure of the catalyst. SEM-EDX analysis was done to confirm the availability and approximate amount of ruthenium ion in the Ru-HT catalyst, and the presence of the ruthenium ion was confirmed tas1.4 wt% (Fig. S3, ESI†).

Fourier transform infrared spectroscopy (FT-IR). The FT-IR spectra of Ru-HT and RRu-HT are displayed in Fig. S4 (ESI†), and show all the characteristic bands of hydrotalcite.[37] The absorption bands at 3600–3500 cm^{-1} and 3000 cm^{-1} are of H-bonding stretching vibrations corresponding to the OH group and interaction between interlayered CO_3^{2-} anions and water molecules, respectively, present in the brucite-like layer. Past reports have showed the use of CO_3^{2-} anions as a carbon source for formic acid.[38] Accordingly, due to the participation of interlayered CO_3^{2-} anions there may be the destruction of free CO_3^{2-} anions during hydrogenation reaction, leading to broadening of the peak at 1647–1350 cm^{-1} in the RRu-HT catalyst.[39] The asymmetric stretching vibration that appeared at 1380–1350 cm^{-1} could be assigned to chelating or interlayer bridging bidentate carbonates. The metal hydroxide vibrational modes of Ru–OH, Al–OH, and Mg–OH in the brucite-type layers may be converted into their respective metal oxide vibrational modes of RuO_2, Al_2O_3 and MgO at 1020–400 cm^{-1}.[22]

Powdered X-ray diffraction (PXRD). The PXRD patterns of Ru-HT and RRu-HT show typical characteristics of hydrotalcite reflections at respective 2θ angles (Fig. S5, ESI†). A good dispersion of Al and Ru in the brucite layers can be seen through the sharp, intense and symmetric peaks 2θ = 10–25 and 2θ = 30–50 diffraction angles.[38] The presence of CO_3^{2-} anions in the interlayer space of HT and Ru-HT was confirmed by the typical basal spacing of the (003) plane; d_{003} = 7.65 Å. The intensity of the characteristic original (003) and (006) planes of HT, which are related to its crystallinity, was observed to decrease after insertion of the Ru ion into the brucite like layer of HT. This decrease in crystallinity could be due to the increase in the number of Ru cations of higher ionic radius than that of the Al cations in the brucite layers. There are extra peaks in the RRu-HT PXRD graph at 2θ = 30–35, 42 and 53, which may be considered as the RuO_2 phase that is generated from the Ru–OH phase of Ru-HT during the catalytic activity corresponding to tetragonal rutile origination the of Ru ion.[40] The absence of CO_3^{2-} anions and the presence of new peaks in the RRu-HT PXRD pattern showing the destruction of interlayered CO_3^{2-} anions from the HT structure suggested the contribution of CO_3^{2-} anions in CO_2 hydrogenation for formic acid formation.[22,40]

X-Ray photoelectron spectroscopy (XPS). The active oxidation state of the Ru ion in Ru-HT catalyst during catalysis was confirmed by X-ray photoelectron spectroscopy (XPS) analysis (Fig. S6, ESI†). Two binding energies were observed in the Ru3d region of Ru-HT, corresponding to the Ru^{II} $3d_{3/2}$ and Ru^{II} $3d_{5/2}$ (spin–orbit separation = 4.1 eV) states at 286.0 eV and 282.83 eV, respectively.[41,42] The values of both binding energies suggest the 2+ oxidation state of Ru ion in the Ru-HT and RRu-HT catalysts, an active catalytic Ru species for the formation of formic acid under optimized reaction conditions.[43]

BET surface area

Comparative values of the pore size, pore volume and the surface area of HT, Ru-HT and RRu-HT show diminished values for the hydrotalcite-HT structure. The pore size and pore volume of HT, Ru-HT and RRu-HT are 26.18 nm and 0.72 cm^3 g^{-1}, 17.4 nm and 0.33 cm^3 g^{-1} and 24 nm and 0.39 cm^3 g^{-1}, respectively. The surface areas of HT, Ru-HT and RRu-HT are 101 m^2 g^{-1}, 76 m^2 g^{-1} and 65 m^2 g^{-1}, respectively. These attenuations in the texture of Ru-HT and RRu-HT propose the superiority of the extent of the size, volume and external surface area of the HT structure in both catalysts by the involvement of Ru. The increase in size and pore volume of RRu-HT and the decrease in surface area after the 7th catalytic cycle lead to the decrease in formic acid production *via* the weakened connection of the Ru ion to the HT layers.

Inductively coupled plasma (ICP)

Inductively coupled plasma (ICP) mass spectrometry analysis was done to find the amount of Ru ion available in the Ru-HT catalyst, followed by the digestion of a known amount of catalyst using *aqua regia* (a mixture of concentrated HCl and HNO_3) and making up the final solution with distilled water to 50 mL in a volumetric flask. The ICP analysis data showed a mean value of 0.487 mg L^{-1} (0.004 mmol) for the Ru ion present in the Ru-HT catalyst (Table 1). When the catalyst starts to drop the formic acid production after the 7th catalytic cycle, the leaching of the Ru ion was checked by ICP and was found to have a negative mean value of −0.114 mg L^{-1}. The reduction in product formation is maybe due to the morphology and structural destruction of the catalyst after the many catalytic cycles.

Kinetic profile

The detailed kinetic study in terms of the formation of the CO_2 hydrogenated product formic acid was carried out at 60 °C, at

Table 1 ICP analysis of Ru-HT and RRu-HT

Entry	Sample	Analyte	Mean (mg L^{-1})
1	Ru-HT[a]	Ru240.3	0.487
2	RRu-HT[b]	Ru240.3	−0.114

[a] Actual loading content of ruthenium ion in the Ru-HT catalyst. [b] Leaching analysis of the ruthenium ion in the RRu-HT catalyst after the 7th catalytic cycle giving a negative mean value.

which the maximum catalytic activity with a TON of 11 389 for formic acid was achieved under 60 bar of CO_2 and H_2 (1 : 1, *p*/*p*) with 60 mL of a mixture of methanol and water (5 : 1, v/v) as the solvent in 24 hours. The kinetic profile for the hydrogenation of CO_2 for the production of formic acid is presented in Fig. 1.

The formic acid formation increased linearly up to 24 hours, and a further increase in the time did not bring about more formation; instead, it started to reach saturation. All other reaction parameters were also taken into account for this kinetic investigation, and the product formation rates were determined appropriately from the slopes of the corresponding plots. The catalyst amount, partial pressure of CO_2 and H_2, total pressure, temperature, agitation speed, reaction volume and volumetric ratio (v/v) of the solvents methanol and water used were considered in an inclusive range for the kinetic exploration by keeping the other reaction parameters constant, while a particular parameter was being studied under the employed reaction conditions. The range of conditions used for kinetic parametric optimization is given in Table 2.

The rates of the formation of formic acid were examined concerning the effects of all the said reaction parameters and were determined using eqn (1) from the plot given in Fig. 1, drawn by increasing concentration of formic acid with time.

$$\text{Rate} = \frac{\mathrm{d}[\text{formic acid}]}{\mathrm{d}t} \quad (1)$$

Table 2 Range of reaction conditions for the kinetic study of CO_2 hydrogenation

Reaction parameter	Range of parameter
Amount of catalyst, mg	20–140
Partial pressure of CO_2, bar	5–40
Partial pressure of H_2, bar	5–40
Total pressure, bar	40–100
Temperature, °C	30–100
Agitation speed, rpm	200–800
Reaction volume, mL	12–60
Methanol : water ratio (v/v)	7 : 1–1 : 5

Dependence of the rate on the amount of catalyst

The relationship between the amount of catalyst and the rate of CO_2 hydrogenation was considered by taking 20–130 mg of catalyst, and the results are given in Fig. 2. The plot of rate *vs.* catalyst amount passes through the origin, indicating that the reaction is completely catalytic under the employed reaction conditions. For the increase in the amount of catalyst from 20 mg, the rate of reaction increased steadily as the total available active sites provide more exposure to bind both gases to itself, leading to an effective increment up to 100 mg of catalyst. On further increasing the catalyst amount a linear increase was not seen and the rate reached saturation. The rate of the formation of formic acid was found to have a first-order dependence on the amount of catalyst.

Dependence of the rate on partial pressures of CO_2 and H_2

The partial pressure of CO_2 was varied from 5 to 40 bar to examine its effect on the rate, and the results are portrayed in Fig. 3. It is very clear from the graph that the rate of formic acid formation was very low at a lower pressure of CO_2, which suggested that an exact and critical amount of CO_2 gas is required along with H_2 gas to get itself appreciably hydrogenated to yield formic acid. The rate of formation was increased after an acute pressure of CO_2 was provided. The determined

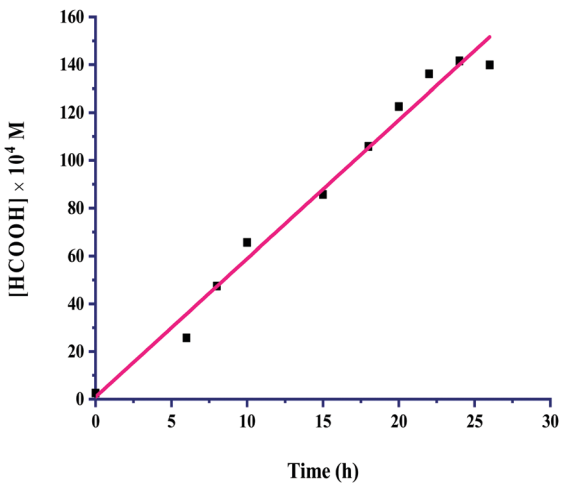

Fig. 1 Kinetic profile: catalyst = 100 mg, pCO_2 = 30 bar, pH_2 = 30 bar, temperature = 60 °C, agitation speed 800 rpm and 60 mL of the solvent of methanol and water (5 : 1, v/v).

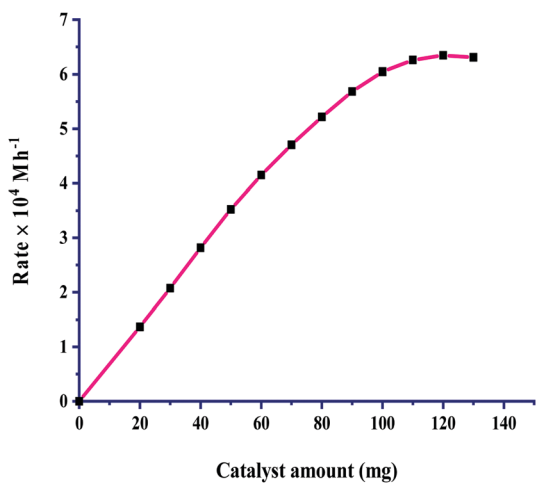

Fig. 2 Dependence of rate on the amount of catalyst: pCO_2 = 30 bar, pH_2 = 30 bar, temperature = 60 °C, agitation speed 800 rpm and 60 mL of a solvent of methanol and water (5 : 1, v/v).

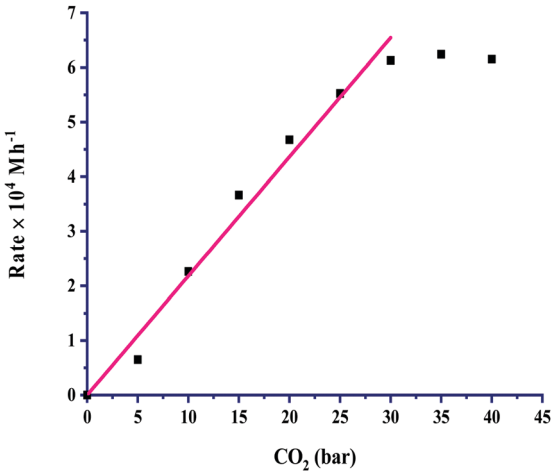

Fig. 3 Dependence of rate on pCO_2: catalyst = 100 mg, pH_2 = 30 bar, temperature = 60 °C, agitation speed 800 rpm and 60 mL of a solvent of methanol and water (5 : 1, v/v).

product formation first reached a maximum level and then started to remain unaffected on further increasing the pressure above 30 bar. On increasing the partial pressure of CO_2 at a constant pressure (30 bar) of H_2, the solubility of H_2 remained constant, and the solubility of CO_2 was increased. The increased solubility of CO_2 with pressure increases the concentration of CO_2 in the reaction. This causes more availability of CO_2 and results in an increased rate of formation of formic acid. First order kinetics were follow in terms of the partial pressure of CO_2 gas. The rate of formation of formic acid was increased with increasing the partial pressure of H_2 from 5 to 30 bar pressure, and a further increase in H_2 pressure provided saturation of the rate. These results, as shown in Fig. 4, indicated that the highest rate was for a 1 : 1 (p/p) ratio of both gases at a total pressure of 60 bar. Similar to the dependence of partial pressure of CO_2, the kinetic dependence in terms of the partial pressure of H_2 was also observed to be first order. The experimental observations for

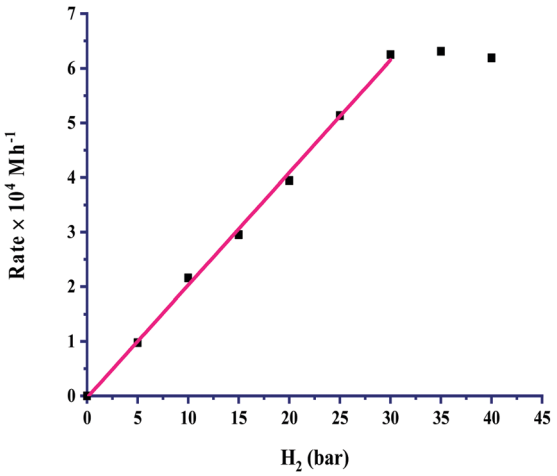

Fig. 4 Dependence of rate on pH_2: catalyst = 100 mg, pCO_2 = 30 bar, temperature = 60 °C, agitation speed 800 rpm and 60 mL of a solvent of methanol and water (5 : 1, v/v).

the effect of the partial pressures of both gases indicated that the 1 : 1 (p/p) ratio is highly favourable for the maximum formation of formic acid under the studied chemical and physical conditions. However, the selectivity of formic acid remained effective with other varied ratios of CO_2 and H_2 gases during partial pressure study.

Dependence of rate on the total pressure, temperature and agitation speed

The dependence of the rate was investigated to observe the effect of total pressure, temperature and agitation speed, and the corresponding results are listed in Table 3.

The total pressure was varied by maintaining the ratio of CO_2 and H_2 at 1 : 1 (p/p) in the pressure range of 40–100 bar, and the corresponding results listed in Table 3 (entries, 1–7) showed a significant effect on the rate. The rates were linearly increased with a pressure of up to 60 bar from 4.18×10^{-4} M h^{-1} to 6.25×10^{-4} M h^{-1} from 30 to 60 bar, and a further increase in total pressure started to attain saturation. On increasing the pressure, the solubilities of both gases increased, which resulted in an increase in the concentration of the gases. Thus the increased concentration of gases enhanced their availability for the reaction and the rates were increased with pressure. The kinetic trend of the total pressure and partial pressures of the individual gases CO_2 and H_2 on the rate was in good agreement of being identical, where the rates were linearly increased up to 60 bar pressure, and above that the rates were unaffected. The dependence of the hydrogenation reaction rate for formic acid on the temperature was studied from near room temperature to high temperatures, in the range of 30 to 100 °C. The solubilities of the gases in the solvent tend to decrease with an increase in temperature. The dependence showed a linear increase in the rate with a rise in temperature from 30 to 60 °C,

Table 3 Effect of total pressure, temperature and agitation speed on the rate of formic acid formation with 100 mg of catalyst and 60 mL of a solvent of methanol and water (5 : 1, v/v)

Entry	pCO_2 (bar)	pH_2 (bar)	Total pressure (bar)	Temp. (°C)	Agitation speed (rpm)	Rate × 10^4 (M h^{-1})
1	20	20	40	60	800	4.18
2	25	25	50	60	800	5.15
3	30	30	60	60	800	6.25
4	35	35	70	60	800	6.30
5	40	40	80	60	800	6.32
6	45	45	90	60	800	6.33
7	50	50	100	60	800	6.33
8	30	30	60	30	800	2.01
9	30	30	60	40	800	3.01
10	30	30	60	50	800	4.00
11	30	30	60	60	800	6.25
12	30	30	60	70	800	6.30
13	30	30	60	80	800	6.34
14	30	30	60	90	800	6.35
15	30	30	60	100	800	6.37
16	30	30	60	60	200	2.96
17	30	30	60	60	300	3.80
18	30	30	60	60	400	4.50
19	30	30	60	60	500	5.02
20	30	30	60	60	600	6.20
21	30	30	60	60	700	6.25
22	30	30	60	60	800	6.26

and then with a further increase in the temperature the rates were found to be saturated. The finding indicated that the solubility effect with the rise in temperature from 30 to 60 °C is not very effective towards reducing the available concentrations of the gases to react to form formic acid and the rates were linearly increased with temperature. The saturating effect of the temperature above 60 °C for the formation of formic acid may be considered for the much lower solubility of CO_2 and H_2 gases at the higher temperature. Under the reaction conditions, lower solubility becomes unable to effectively enhance the available concentration of these gases. The Arrhenius plot drawn in the temperature range of 30 to 60 °C shows a good linear fit and was used for evaluating the activation parameters (Fig. 5). The determined activation parameters of E_a = 34.5 ± 2.5 kJ mol^{-1}, $\Delta H^{\#}$ = 32 ± 2.5 kJ mol^{-1} and $\Delta S^{\#}$ = −384 ± 5 J deg^{-1} mol^{-1} indicated that both the activation enthalpy and the highly negative entropy associated with hydrogenation were highly favourable for the activation of CO_2 and H_2 for the selective formation of formic acid. The reported activation parameters for the Rh-hydrotalcite (Rh-HT)-based catalyst, for the catalyzed hydrogenation of CO_2 to formic acid, are E_a = 33.5 ± 2.5 kJ mol^{-1}, $\Delta H^{\#}$ = 30.9 ± 2.5 kJ mol^{-1} and $\Delta S^{\#}$ = −275 ± 5 J deg^{-1} mol^{-1}.[18]

The activation enthalpies are almost comparable for the Ru-HT and Rh-HT catalytic systems; however, the entropy of activation is observed to be remarkably much more favourably associated with Ru-HT. An almost closer activation energy, 31 kJ mol^{-1}, is reported for Ru-based catalysts under homogeneous conditions up to a slightly lower temperature of 40 °C.[44] G. Laurenczy *et al.* investigated hydrogenation of CO_2 to formic acid catalyzed by Ru-complexes and obtained an activation enthalpy of 96 kJ mol^{-1} under homogeneous conditions, studying the reaction in the temperature range of 23–90 °C.[31] These observations indicated that heterogeneous catalyst systems performing well towards the activation enthalpies associated with CO_2 hydrogenation, and that the enthalpies are effectively reduced thereby making the reaction more favourable.

The dependence of the rate on the agitation speed in the range of 200–800 rpm (Table 3, entries 16–22) showed that the rate significantly increased for 200–500 rpm, from 2.96 × 10^{-4} M h^{-1} to 5.02 × 10^{-4} M h^{-1}, respectively, and on further increasing the agitation speed the rates followed a steady state. At the lower agitation speed, the initial concentration of dissolved gases was less, which indicates a diffusion-controlled reaction; hence, the rate of reaction increases. Furthermore, on increasing the agitation speed, although the initial concentrations of dissolved gases are significantly increased and the concentration of dissolved gases in the reaction mixture becomes higher, the rate remained unaffected. Hence an agitation speed above 500 rpm has a negligible effect upon the reaction rate, which indicated the absence of mass transfer resistance and that the reaction is under the kinetic regime. To ensure a purely kinetic regime, all the experiments were preferentially performed at 800 rpm. The use of finely powdered Ru-HT catalyst eliminated the effect of internal diffusion during the kinetic study. The particle size of the hydrotalcite-based ruthenium catalyst is reported to be in the order of a nanometer.[45] Also the pore size of Ru-HT is 17.4 nm, which is bigger than that of general mesoporous materials, enabling easy ingress of the reactants and egress of the products. This is also in line with the observations on the Cu-hydrotalcite catalyst, where the particle size of below 100 micrometers is reported to be in the kinetic regime by eliminating internal diffusion.[46] The stability of the product was observed to be well maintained over the entire range of the total applied pressure, temperature and agitation speed.

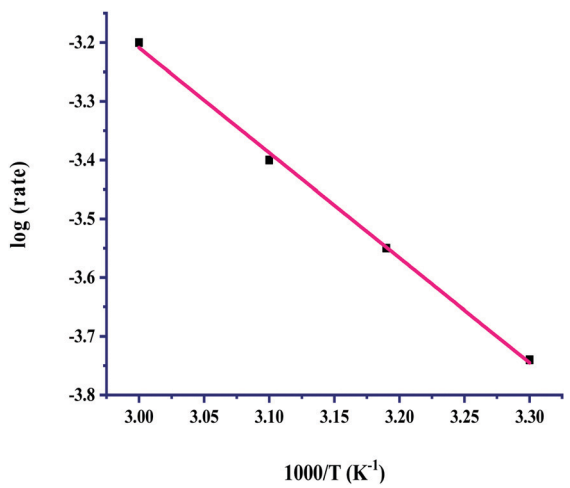

Fig. 5 Arrhenius plot of log rate *vs.* 1/*T* for the formation of formic acid.

Dependence of rate on reaction volume and v/v ratio of methanol and water

The hydrogenation of CO_2 was carried out by varying the reaction volume fivefold, from 12 to 60 mL by keeping the ratio of methanol/water, 5 : 1 (v/v), and the corresponding results are given in Table 4. The reaction volume and the respective solubilities of the CO_2 and H_2 gases in the used solvent have remarkably contributed to influence the rate. The solubilities in mmol L^{-1} at 1 atm pressure and 25 °C, of H_2 and CO_2 in water, are 0.68 and 58.8, respectively.[47] Under these conditions, the solubilities of H_2 and CO_2 in methanol are 3.86 and 137.8, respectively. Solubilities of both gases are appreciably higher in methanol. In a comparison of hydrogen, the solubility of CO_2 is much higher in both the solvents water and methanol. CO_2 is a polar solute with a partial positive charge on the carbon and a partial negative charge on the oxygen, and water and methanol are polar solvents that greatly favour the solubility.

The rate of formation was linearly increased (Table 4, entries 1–9) with an increase in the reaction volume. With 12 mL of the solvent, the rate was 1.22 × 10^{-4} M h^{-1}, which was appreciably increased to 6.25 × 10^{-4} M h^{-1} with 60 mL of solvent. The larger volume of solvent was found to be very effective to dissolve the gases, which allows for higher concentrations of CO_2 and H_2 in the reaction system. Thus more solubility in the larger reaction volume enhances the available concentrations of these gases, resulting in an increased rate.

To observe the effect of the ratio of the used solvent on the rate, the ratio (v/v) of methanol and water was suitably varied

Table 4 Effect of reaction volume and v/v ratio of methanol and water on the rate of formic acid formation with 100 mg of catalyst, pCO_2 = 30 bar, pH_2 = 30 bar, temperature = 60 °C and agitation speed = 800 rpm

Entry	Methanol, mL	Water, mL	Rean volume, mL	Methanol/water ratio (v/v)	Rate × 10^4 M h^{-1}
1	10	2	12	5 : 1	1.22
2	15	3	18	5 : 1	1.85
3	20	4	24	5 : 1	2.50
4	25	5	30	5 : 1	3.12
5	30	6	36	5 : 1	3.66
6	35	7	42	5 : 1	4.37
7	40	8	48	5 : 1	4.83
8	45	9	54	5 : 1	5.47
9	52.5	7.5	60	7 : 1	6.26
10	51.5	8.5	60	6 : 1	6.27
11	50	10	60	5 : 1	6.25
12	40	20	60	4 : 2	5.83
13	30	30	60	3 : 3	5.42
14	20	40	60	2 : 4	4.16
15	10	50	60	1 : 5	3.33
16	60	0	60	—	2.99
17	0	60	60	—	1.02

from 7 : 1 to 1 : 5 by maintaining the total reaction volume 60 mL under identical conditions of the other parameters, and the results are listed in Table 4. A decreasing trend in the rate (Table 4, entries 10–15) was observed with a decreasing volume of methanol from 5 : 1 to 1 : 5. The maximum rate (6.25 × 10^{-4} M h^{-1}) was with the ratio of 5 : 1, and on further increasing the volume of methanol the rates were almost constant at the ratios of 6 : 1 and 7 : 1 (Table 4, entries 9 and 10) indicating that the ratio of 5 : 1 is effective to maintain the best performance of the catalyst to produce formic acid. The rate using only methanol as a solvent without water was 2.99 × 10^{-4} M h^{-1} (Table 4, entry 16), and with only water (Table 4, entry 17) it was 1.02 × 10^{-4} M h^{-1}. The higher rate using only methanol as the solvent is due to the higher solubilities of both the gases in it. An effective synergy of the mixed methane–water solvent was observed to enhance the rate. These rates obtained from the individual solvents methanol and water were effectively increased with the mixed solvent to 6.25 × 10^{-4} M h^{-1} at the ratio of 5 : 1.

Reaction mechanism

Based on the kinetic first-order dependence in terms of the amounts of the catalyst and partial pressures of CO_2 and H_2 and the experimental observations, a reaction mechanistic route of CO_2 hydrogenation to formic acid over Ru-HT is proposed in Scheme 1 *via* two plausible reaction pathways.

The first one is a stepwise mechanism in which the inserted metal ion of Ru-HT (**1**) triggers the H_2 molecule to form hydride bonds with the ruthenium ion for the formation of the intermediate (**2**). This is in line with the experimentally observed first-order kinetic dependence with respect to the catalyst and H_2. The reactivity of H_2 facilitates its interaction to react with the catalyst first. Based on the first-order dependence with CO_2 and comparatively lower reactivity of it, in the next step, the reaction proceeds with the absorption of CO_2 on the surface of the catalyst and the bond between carbon and the hydride

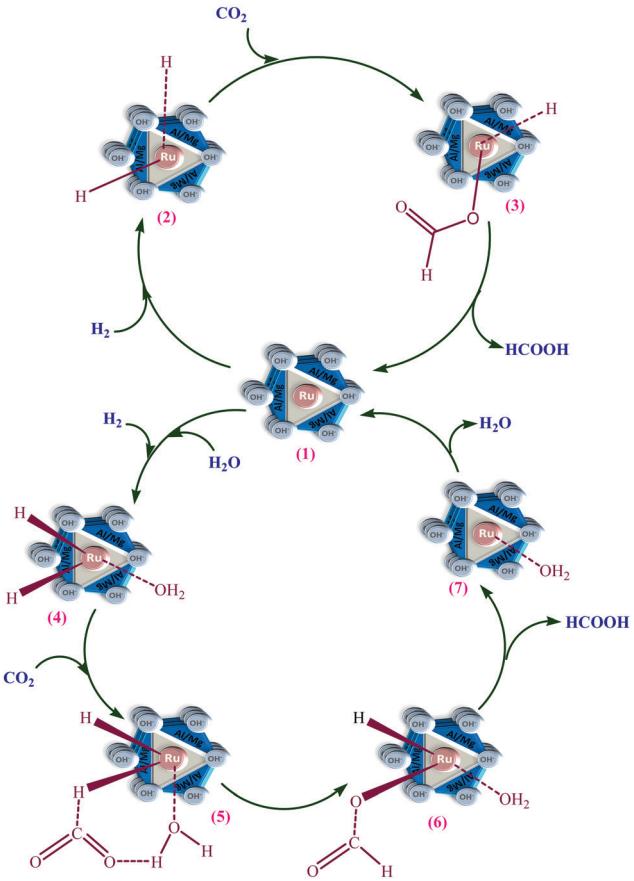

Scheme 1 Proposed reaction mechanisms of CO_2 hydrogenation to formic acid over Ru-HT.

of the metal ion for the formation of formate ion with the metal.

The second one is based on the contribution of water to the reaction, which is more precise concerning an effectually active solvent molecule in the mechanistic path. Consequently, the dissociation of the coordinated water increases the scope for the successive insertion and coordination of CO_2. The reaction proceeds quickly and easily since H_2 gets activated first by the catalyst (**1**) to form Ru–H_2 (Ru-dihydride) (**2**) under the applied reaction conditions because the reactivity of CO_2 is less than that of H_2.[48–51] The reaction of Ru-hydride (**2**) with CO_2 through the insertion of CO_2 into one of the hydride bonds forms the intermediate formate (**3**). In the rate-determining step, the reductive elimination of formate (**3**) yields formic acid and the coordinatively unsaturated ruthenium species.[36,48–50] To complete the catalytic cycle, the rapid oxidative addition of dihydrogen regenerates the catalyst (**1**).

The presence of water with methanol enhanced the formation of formic acid. However, the solubility of both gases in water is significantly less than that of methanol.[47] On the one hand, the solubility of CO_2 is more than twice, and that of H_2 is more than 5 times greater in methanol than it is in water. On the other hand, five times excess volume of methanol with respect to water is taken during the catalytic reaction. Thus, in the volume of both solvents taken, in terms of the solubility, the contribution

of methanol as a solvent is greater to enhance the reaction rate. Here the role of water to enhance the rate of formation is small concerning its solvent properties due to the higher solubility of both gases in methanol compared with water. The contribution of water appeared to be more specific regarding the molecular effect functioning in the mechanistic path. During the reaction, the molecular effect in terms of the operative mechanism was contributed by molecular water, which increases the dissociation of the coordinated water and eases the consequential insertion and coordination of CO_2 to a high amount.

The aquated Ru intermediate (**4**) reacted with one of the oxygens of CO_2 for its coordination *via* the H-bonding interaction of the water, which caused the formation of the next intermediate (**5**). The insertion of CO_2 into the Ru–H bond during formate formation (**6**) caused stabilization of the transition state between intermediates (**5**) and (**6**). This stabilization polarizes the fragment of CO_2 by enhancing the electrophilicity of CO_2 on the carbon and the susceptibility of hydride transfer from Ru to yield formic acid along with the intermediate (**7**). This intermediate (**7**), undergoing rapid oxidative addition of dihydrogen, formed the catalyst (**1**).

Conclusions

Kinetic, thermodynamic and mechanistic aspects of the ruthenium-inserted hydrotalcite (Ru-HT) heterogeneous catalyst were investigated for hydrogenation of CO_2 for the selective formation of formic acid. The rates were determined in terms of the formation of formic acid. Kinetic investigations were performed as a function of the amount of catalyst, the partial pressures of the individual gases CO_2 and H_2, total pressure, agitation speed, temperature, reaction volume and the volumetric ratio (v/v) of the used mixed solvent mixture of methanol and water. The rate of formation of formic acid depended significantly on all these studied parameters. The rate of formation followed first-order kinetics with respect to the amount of catalyst and the partial pressures of the reacting gases. All the parameters were varied over a wide range of values to observe their effects on the rate and for their kinetic parametric optimisation. The maximum rate of 6.25×10^{-4} M h^{-1} was observed under the following optimised kinetic reaction conditions: 100 mg of catalyst, pCO_2 = 30 bar, pH_2 = 30 bar, temperature = 60 °C, agitation speed = 800 rpm and a methanol–water (v : v = 5 : 1) solvent. The activation enthalpy and entropy determined from the temperature dependence were very favourable under the employed reaction conditions. Based on the kinetic findings and the experimental results, two reaction mechanisms for the Ru-HT-catalyzed synthesis of formic acid were proposed, wherein the molecular effect of water was observed to be efficiently operative.

Conflicts of interest

There are no conflicts to declare.

Acknowledgements

CSMCRI communication No. IMC 03, CSIR-CSMCRI – 155/2018. The authors thank Council of Scientific and Industrial Research (CSIR), New Delhi, India for the financial support through Network Project on Clean Coal Technology (Tap Coal, CSC 0102) and Analytical Division and Central Instrumentation Facility of CSIR Central Salt and Marine Chemicals Research Institute, Bhavnagar, for providing instrumental analysis.

Notes and references

1 (*a*) W.-H. Wang, Y. Himeda, J. T. Muckerman, G. F. Manbeck and E. Fujita, *Chem. Rev.*, 2015, **115**, 12936; (*b*) M. Aresta, A. Dibenedetto and A. Angelini, *Chem. Rev.*, 2014, **114**, 1709–1742; (*c*) G. Centi, E. A. Quadrelli and S. Perathoner, *Energy Environ. Sci.*, 2013, **6**, 1711; (*d*) M. Grasemann and G. Laurenczy, *Energy Environ. Sci.*, 2012, **5**, 8171; (*e*) C. Federsel, R. Jackstell and M. Beller, *Angew. Chem., Int. Ed.*, 2010, **49**, 6254 (*Angew. Chem.*, 2010, **122**, 6392); (*f*) Y. Inoue, H. Izumida, Y. Sasaki and H. Hashimoto, *Chem. Lett.*, 1976, 863.

2 J. Z. Zhang, Z. Li, H. Wang and C. Y. Wang, *J. Mol. Catal. A: Chem.*, 1996, **112**, 9.

3 R. S. Shukla, S. D. Bhatt, R. B. Thorat and R. V. Jasra, *Appl. Catal., A*, 2005, **294**, 111.

4 C. Fellay, P. J. Dyson and G. A. Laurenczy, *Angew. Chem., Int. Ed.*, 2008, **47**, 3966.

5 (*a*) Y. Kiso and K. Saeki, *Jpn Pat.*, 5236617, 1977; (*b*) J. Z. Zhang, Z. Li, H. Wang and C. Y. Wang, *J. Mol. Catal. A: Chem.*, 1996, **112**, 9.

6 W. Gan, P. J. Dyson and G. Laurenczy, *ChemCatChem*, 2013, **5**, 3124.

7 T. Schaub and R. A. Paciello, *Angew. Chem., Int. Ed.*, 2011, **50**, 7278.

8 G. A. Olah, A. Goeppert and G. K. Surya Prakash, *Beyond Oil and Gas: The Methanol Economy*, Weinheim, Wiley-YCH, 2006.

9 S. Saeidi, N. A. S. Amin and M. R. Rahimpour, *J. CO2 Util.*, 2014, **5**, 66.

10 R. W. Dorner, D. R. Hardy, F. W. Williams and H. D. Willauer, *Energy Environ. Sci.*, 2010, **3**, 884.

11 (*a*) J. Klankermayer, S. Wesselbaum, K. Beydoun and W. Leitner, *Angew. Chem., Int. Ed.*, 2016, **55**, 7296 (*Angew. Chem.*, 2016, **128**, 7416); (*b*) J. Klankermayer and W. Leitner, *Philos. Trans. R. Soc., A*, 2016, **374**, 20150315; (*c*) W. Leitner, *Angew. Chem., Int. Ed. Engl.*, 1995, **34**, 2207 (*Angew. Chem.*, 1995, **107**, 2391); (*d*) H. Hayashi, S. Ogo and S. Fukuzumi, *Chem. Commun.*, 2004, 2714; (*e*) W. Leitner, E. Dinjus and F. Gaßner, in *CO2 Chemistry-Aqueous-Phase Organometallic Catalysis*, ed. B. Cornils and W. A. Hermann, Wiley-VCH, Weinheim, 1998, p. 488.

12 M. S. Maru, P. Patel, N. H. Khan and R. S. Shukla, *Curr. Catal.*, 2020, **9**, 59.

13 (*a*) P. Patel, S. Nandi, M. S. Maru, R. I. Kureshy and N. H. Khan, *J. CO2 Util.*, 2018, **25**, 310; (*b*) M. S. Maru,

S. Ram, R. S. Shukla and N. H. Khan, *J. Mol. Catal.*, 2018, **446**, 23.
14 M. S. Maru, S. Ram, J. H. Advani and R. S. Shukla, *ChemistrySelect*, 2017, **2**, 3823.
15 M. D. Khokhar, R. S. Shukla and R. V. Jasra, *J. Mol. Catal.*, 2015, **400**, 1.
16 M. D. Khokhar, R. S. Shukla and R. V. Jasra, *React. Kinet., Mech. Catal.*, 2015, **114**, 265.
17 (*a*) N. Sudheesh and R. S. Shukla, *Appl. Catal., A*, 2014, **473**, 116; (*b*) N. Sudheesh and R. S. Shukla, *Appl. Catal., A*, 2013, **453**, 159.
18 (*a*) N. Sudheesh, J. N. Parmar and R. S. Shukla, *Appl. Catal., A*, 2012, **415–416**, 124; (*b*) N. Sudheesh, A. K. Chaturvedi and R. S. Shukla, *Appl. Catal., A*, 2011, **409–410**, 99.
19 (*a*) N. Sudheesh, S. K. Sharma, R. S. Shukla and R. V. Jasra, *J. Mol. Catal. A: Chem.*, 2010, **316**, 23; (*b*) N. Sudheesh, S. K. Sharma, R. S. Shukla and R. V. Jasra, *J. Mol. Catal. A: Chem.*, 2008, **296**, 61.
20 S. K. Sharma, R. S. Shukla, P. A. Parikh and R. V. Jasra, *J. Mol. Catal.*, 2009, **304**, 33.
21 V. K. Srivastava, S. K. Sharma, R. S. Shukla and R. V. Jasra, *Ind. Eng. Chem. Res.*, 2008, **47**, 3795.
22 (*a*) S. K. Sharma, V. K. Srivastava, R. S. Shukla, P. A. Parikh and R. V. Jasra, *New J. Chem.*, 2007, **31**, 277; (*b*) R. V. Jasra, V. K. Srivastava, R. S. Shukla, H. C. Bajaj and S. D. Bhatt, *US Pat.*, 7294745 B2, 2007; (*c*) V. K. Srivastava, S. K. Sharma, R. S. Shukla and R. V. Jasra, *Catal. Commun.*, 2006, **7**, 879.
23 F. Basile, L. Basini, G. Fornasari, M. Gazzano, F. Trifiro and A. Vaccari, *Chem. Commun.*, 1996, 2435.
24 K. Kaneda, T. Yamashita, T. Matsushita and K. Ebitani, *J. Org. Chem.*, 1998, **63**, 1750.
25 T. Matsushita, K. Ebitani and K. Kaneda, *Chem. Commun.*, 1999, 265.
26 (*a*) K. Motokura, D. Nishimura, K. Mori, T. Mizugaki, K. Ebitani and K. Kaneda, *J. Am. Chem. Soc.*, 2004, **126**, 5662; (*b*) K. Motokura, T. Mizugaki, K. Ebitani and K. Kaneda, *Tetrahedron Lett.*, 2004, **45**, 6029.
27 F. Basile, G. Fornasari, M. Gazzano and A. Vaccari, *J. Mater. Chem.*, 2002, **12**, 3296.
28 B. B. İsmail, Y. Mehmet, S. K. Gülşah and B. Ahmet, *Turk. J. Chem.*, 2020, **44**, 364.
29 J. A. Martins, A. C. Faria, M. A. Soria, C. V. Miguel, A. E. Rodrigues and L. M. Madeira, *Catalysts*, 2019, **9**, 1008.
30 W. Wang, S. Wang, X. Ma and J. Gong, *Chem. Soc. Rev.*, 2011, **40**, 3703.
31 S. Moret, P. J. Dyson and G. Laurenczy, *Nat. Commun.*, 2014, **5**, 1.
32 G. Laurenczy, F. Joó and L. Nádasdi, *Inorg. Chem.*, 2000, **39**, 5083.
33 A. Xin, Z. Yizan, Z. Qiang and W. Jinfu, *Chin. J. Chem. Eng.*, 2009, **17**, 88.
34 J. Ye, C.-J. Liu, D. Mei and Q. Ge, *J. Catal.*, 2014, **317**, 44.
35 R. J. Berger, E. H. Stitt, G. B. Martin, F. Kapteijn and J. A. Moulijn, *CATTECH*, 2001, **5**, 30.
36 (*a*) R. Salomão, L. M. Milena, M. H. Wakamatsu and V. C. Pandolfelli, *Ceram. Int.*, 2011, **37**, 3063; (*b*) S. K. Sharma, P. A. Parikh and R. V. Jasra, *J. Mol. Catal. A: Chem.*, 2010, **317**, 27.
37 F. Cavani, F. Trifiro and A. Vaccari, *Catal. Today*, 1991, **11**, 173.
38 G. H. Gunasekar, K. Park, K.-D. Jung and S. Yoon, *Inorg. Chem. Front.*, 2016, **3**, 882.
39 B. Wiyantoko, P. Kurniawati, T. E. Purbaningtias and I. Fatimah, *Procedia Chem.*, 2015, **17**, 21.
40 (*a*) S. Pichaikaran and P. Arumugam, *Green Chem.*, 2016, **18**, 2888; (*b*) Md. T. Uddin, Y. Nicolas, C. Olivier, L. Servant, T. Toupance, S. Li, A. Klein and W. Jaegermann, *Phys. Chem. Chem. Phys.*, 2015, **17**, 5090; (*c*) N. Ullah and S. Omanovic, *Mater. Chem. Phys.*, 2015, **159**, 119; (*d*) A. Ballarini, P. Benito, G. Fornasari, O. Scelza and A. Vaccari, *Int. J. Hydrogen Energy*, 2013, **38**, 15128.
41 (*a*) J. F. Moulder, W. F. Stickle, P. E. Sobol and K. D. Bomben, *Handbook of X-ray Photoelectron Spectroscopy: A Reference Book of Standard Spectra for Identification and Interpretation of XPS Data*, PerkinElmer, Boca Raton, FL, 1992; (*b*) R. E. Shepherd, A. Proctor, W. W. Henderson and T. K. Myser, *Inorg. Chem.*, 1987, **26**, 2440.
42 (*a*) A. Jana, J. Mondal, P. Borah, S. Mondal, A. Bhaumik and Y. Zhao, *Chem. Commun.*, 2015, **5151**, 10746; (*b*) D. J. Morgan, *Surf. Interface Anal.*, 2015, **47**, 1072.
43 (*a*) A. Dibenedetto, P. Stufano, F. Nocito and M. Aresta, *ChemSusChem*, 2011, **4**, 1311; (*b*) S. Ogo, R. Kabe, H. Hayashi, R. Harada and S. Fukuzumi, *Dalton Trans.*, 2006, 4657; (*c*) Y. Ohnishi, T. Matsunaga, Y. Nakao, H. Sato and S. Sakaki, *Organometallics*, 2006, **25**, 3352; (*d*) Y. Ohnishi, T. Matsunaga, Y. Nakao, H. Sato and S. Sakaki, *J. Am. Chem. Soc.*, 2005, **127**, 4021.
44 M. M. Taquikhan, S. B. Halligudi and S. Shukla, *J. Mol. Catal.*, 1989, **57**, 47.
45 J. A. Martins, A. C. Faria, M. A. Soria, C. V. Migual, A. E. Rodrigues and L. M. Maderia, *Catalysts*, 2019, **9**, 1008.
46 P. Kumar, R. C. Korosec and U. L. Stanger, *J. Colloid Interface Sci.*, 2021, **585**, 549.
47 H. Stephen and T. Stephen, *Solubilities of Inorganic and Organic Compounds part I and II*, Pergamon Press, New York, 1963, vol. I.
48 (*a*) P. G. Jessop, F. Joý and C.-C. Tai, *Coord. Chem. Rev.*, 2004, **248**, 2425; (*b*) P. G. Jessop, T. Ikariya and R. Noyori, *Chem. Rev.*, 1995, **95**, 259.
49 F. Joo, *Aqueous Organometallic Catalysis*, Kluwer Academic Publishers, Dordrecht, 2001.
50 (*a*) W. Leitner, E. Dinjus and F. GaBtier, *J. Organomet. Chem.*, 1994, **475**, 257; (*b*) F. Gassner and W. Leitner, *J. Chem. Soc., Chem. Commun.*, 1993, 1465; (*c*) P. G. Jessop, T. Ikariya and R. Noyori, *Nature*, 1994, **368**, 231.
51 J. C. Tsai and K. M. Nicholas, *J. Am. Chem. Soc.*, 1992, **114**, 5117.